Exciton Coupling and Dipolar Correlations in a Columnar Liquid Crystal: Photophysics of a Bent-Rod Hexacatenar Mesogen

Igor A. Levitsky, Keiki Kishikawa, S. Holger Eichhorn, and Timothy M. Swager*

Contribution from the Department of Chemistry and Center for Materials Science and Engineering, Massachusetts Institute of Technology, Cambridge, Massachusetts 02139

Received November 8, 1999

Abstract: A novel bent-rod hexacatenar liquid crystal is reported that displays a hexagonal columnar (Col_h) phase. The organization of conjugated hexacatenar mesogens in the columnar phase is of interest for their anisotropic electronic properties. The emissive nature of the mesogens varies over the temperature range of the Col_h phase and the spectral shifts were analyzed in terms of an exciton-coupling model. The variation of the emission band in this phase is consistent with varying degrees of rotational disorder between the mesogens. The bent-rod shape and highly dipolar nature of the liquid crystal core (mesogen) promotes (as suggested by computation, X-ray diffraction, and photophysical studies) a high degree of antiparallel intermolecular correlations between nearest neighbors. The antiparallel organization is novel and differs from structures previously identified in other polycatenars. These studies illustrate the utility of the exciton-coupling model to probe the nature and degree of intermolecular correlations in highly dipolar liquid crystals.

Introduction

The liquid crystalline state offers a wealth of possibilities for the assembly of molecules with designed electronic or magnetic properties into organized structures, exhibiting novel bulk properties. The realization of this potential requires a detailed understanding of the dynamics and organizational phenomenon to allow predictions and the design of novel photonic and electronic materials. However, the disordered nature of liquid crystalline systems makes detailed investigations of structure challenging. Clearly, short-range correlations between molecules in liquid crystalline phases are important and are necessary to produce cooperative phenomena such as optical biaxiality and ferroelectricity. As a result, new ways to analyze intermolecular organizations are of particular importance. Dipolar correlations between mesogens are most often investigated by dielectric spectroscopy. Other approaches for the elucidation of the local intermolecular correlations of a liquid crystalline phase include combinations of NMR, X-ray structural analysis, and dilatometry.[1]

Columnar liquid crystals often display a high degree of electronic communication between mesogenic cores within a column, and these systems have been generally viewed as efficient charge transport and energy transfer conduits.[2] Typically discoid molecules arrange into highly anisotropic columnar stacks with close intermolecular stacking, 3−4 Å, of unsaturated cores and much greater distances separating the columns (20−50 Å, depending on the length of the side-chains). Approaches to the design of specific properties in columnar phases include the use of molecular shape,[3] dative bonding,[4] and strong dipolar interactions.[5] In designing systems the most important goal is to create intermolecular associations that support optimal long-range collective properties including electronic conductivity, energy transport, ferroelectricity, and optical biaxiality. In considering shape as a design element we have been particularly interested in a class of compounds called polycatenars.[6] Polycatenars are liquid crystals with rodlike (calamitic) mesogenic cores and multiple side-chains attached to their terminus.

Our present investigations focus on detailed photophysical studies and an analysis of exciton coupling[7,8] of a novel electronically active hexacatenar columnar liquid crystal with a bent-rod structure. The combination of the bent-rod shape and a large lateral dipole are intended to produce highly correlated mesogen assemblies with optimal energy transport characteristics. To date photophysical studies of liquid crystals have seen limited investigation.[9−16] There still remains much to be learned

(1) See contributions in: *Handbook of Liquid Crystals*; Demus, D., Goodby, J., Gray, G. W., Spiess, H.-W., Vill, V., Eds.; Wiley-VCH: Weinheim, 1998; Vol. 1, Chapter 7.

(2) *Handbook of Liquid Crystals*; Demus, D., Goodby, J., Gray, G. W., Spiess, H.-W., Vill, V., Eds.; Wiley-VCH: Weinheim, 1998; Vol. 2b.

(3) Demus, D. *Liq. Cryst.* **1989**, *5*, 75−110.

(4) (a) Serrette, A. G.; Swager, T. M. *Angew. Chem., Int. Ed. Engl.* **1994**, *33*, 2342−5. (b) Serrette, A. G.; Swager, T. M. *J. Am. Chem. Soc.* **1993**, *115*, 5, 8879−8880.

(5) Kishikawa, K.; Harris, M. C.; Swager, T. M. *Chem. Mater.* **1999**, *11*, 867−871.

(6) Hexacatenar refers to a mesogen with six side chains. For reviews see: (a) Malthête, J.; Nguyen, H. T.; Destrade, C. *Liq. Cryst.* **1993**, *13*, 171−187. (b) Nguyen, H. T.; Destrade, C.; Malthête, J. *Handbook of Liquid Crystals*; Demus, D., Goodby, J., Gray, G. W., Spiess, H.-W., Vill, V., Eds.; Wiley-VCH: Weinheim, 1998; Vol. 2b, Chapter 12.

(7) Kasha, M.; Rawls, H. R.; El-Bayoumi, M. A. *Pure Appl. Chem.* **1965**, *11*, 371

(8) Kasha, M. In *Spectroscopy of the Excited State*; Di Bartolo, B., Ed.; Plenum Press: New York, 1976.

(9) Markovitsi, D.; Lécuyer, I.; Clergeot, B.; Jallabert, C.; Strzelecka, H.; Veber, M. *Liq. Cryst.* **1989**, *6*, 83.

(10) Blanzat, B.; Barthou, C.; Tercier, N.; André, J.-J.; Simon, J. *J. Am. Chem. Soc.* **1987**, *109*, 6193.

(11) Blasse, G.; Dirksen, G. J.; Meijerink, A.; Van der Pol, J. F.; Neeleman, E.; Drenth, W. *Chem. Phys. Lett.* **1989**, *154*, 420.

(12) Markovitsi, D.; Lecuyer, I.; Simon, J. J. *J. Phys. Chem.* **1991**, *95*, 3620.

(13) Gregg, B. A.; Fox, M. A.; Bard, A. J. *J. Phys. Chem.* **1989**, *93*, 4227.

(14) Ecoffet, C.; Markovitsi, D.; Millié, P.; Lemaistre, *Chem. Phys.* **1993**, *177*, 629.

(15) Markovitsi, D.; Germain, A.; Millié, P.; Lécuyer, P.; Gallos, L. K.; Argyrakis, P.; Bengs, H.; Ringsdorf, H. *J. Phys. Chem.* **1995**, *99*, 1005.

(16) Hoag, B. P.; Gin, D. L. *Adv. Mater.* **1998**, *10*, 1546.

10.1021/ja993947d CCC: $19.00
Published on Web 03/02/2000

from analysis of the photophysics of these materials. A particularly useful approach is the exciton coupling model of Kasha, which has long been used to understand molecular aggregates.[7] Herein we use exciton coupling analysis as an additional tool for the analysis of pairwise organizations in novel mesophases. Previous studies by Markovitsi and co-workers provide a foundation for the study of the photophysical properties of discotic liquid crystals.[9,12,14,15] In these studies a combination of quantum chemical calculations with an exciton theory show good agreement between spectroscopic modeling of columnar liquid crystalline phases and experimental data.[14,15] Detailed photophysical studies have been performed on columnar phases of disklike molecules such as porphyrin,[13] phthalocyanine,[10,11] triarylpryilium,[14] and triphenylene[15] structures. In this contribution we extend these methods to the study of molecules with a bent-rod shape and a highly dipolar nature that produces strong orientational correlations between nearest neighbor mesogens. Our combined photophysical, X-ray diffraction, and computational analysis of these liquid crystals support a new model for the organization of hexacatenar liquid crystals.

Results and Discussion

Compounds **2**[5] and **3**[10] were synthesized as previously reported, and the synthesis of **1** was performed by adaptation of published procedures.[5] Compound **1** melts at 43 °C to give a well-defined hexagonal columnar (Col_h) liquid crystal phase. This Col_h phase is stable with continued heating until 69 °C

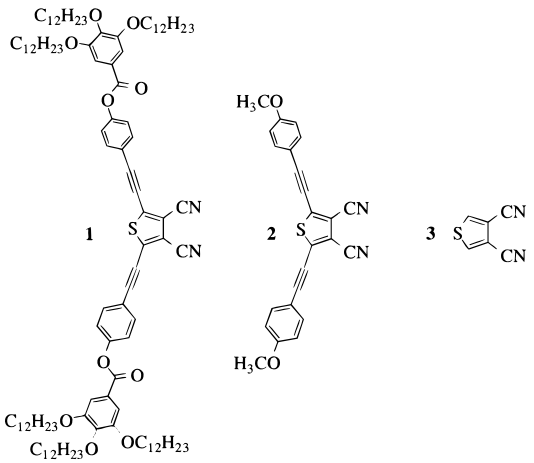

where the compound enters its isotropic state. The optical texture shown in Figure 1 is characteristic of a hexagonal arrangement of columns with regions of uniform extinction, and fan-shaped features that had extinction brushes aligned with the polarizers. Additionally, small amounts of rectilinear defects were observed. The liquid crystalline phase of **1** at 64 °C displayed three distinct reflections in the small-angle X-ray region (d = 38.39, 22.03, and 19.12 Å) and two reflections in the wide angle region (7.06 (broad) and 4.5 Å (diffuse)). The small-angle peaks index to the (100), (110), and (200) reflections of a two-dimensional hexagonal lattice confirming the Col_h assignment. In the wide-angle region, the correlation length of 7.06 Å represents the spacing between every second mesogen unit within a column. Similar features have been previously observed by our group in other highly correlated columnar mesogens having antiparallel correlation between nearest neighbors.[17] However, in this case a first-order reflection for the stacking of the central aromatic units at about 7.06/2 Å was not unambiguously observed. The wide-angle "halo" at 4.5 Å is typical for molten aliphatic chains and proves the presence of a liquid crystalline state. The hexagonal lattice parameter was calculated to 44.33 Å, and a molecular volume of 5956 Å^3 can be derived from this taking 3.5 Å as intracolumnar spacing. These values are in good agreement with computational results and the molecular dimensions found in single crystals of short-chain derivatives.[5] These structural studies prompted us to consider that the columnar packing of **1** is different from the proposed organization of Col_h phases of conventional hexacatenar mesogens where two to three molecules assemble into "smectoid" or layered aggregates within the column (Scheme 1).[6] The bent-rod shape and the strong lateral dipole of **1** likely have a distinct influence on the nearest neighbor interaction, which in turn influences the overall supramolecular structure. A more circular space filling structure than shown in Scheme 1 is likely when one considers that other rotational conformations of the benzoate esters are present.

The fluorescence and absorption spectra of three related compounds, **1**, **2**, and **3**, in chloroform are shown in Figure 2. Compounds **1** and **2** have a similar extended chromophore whereas **3** has an absorption only at very high energy, thus confirming that the electronic properties of **1** and **2** are dictated by the extended chromophore. Considering the high electron affinity of the nitrile groups, we anticipated that both **1** and **2** should have charge-transfer character in their excited state. Consistent with this view, the absorption edge of **2** is shifted slightly to the red of **1**. This is due to the fact that the terminal methoxy substituent in **2** is a better donor than the ester moiety in **1**. Hence the excited state reduces the electron density on the phenyl rings and increases the negative charge on the nitrile groups. It is also important to note that the similarity in shape of the absorption and emission spectra of **1** and **2** confirms the validity of our comparisons.

Having established the nature of the chromophore, we can now estimate the length of the transition dipole moment, l, to be between 10 and 25 Å. The value of the transition dipole moment, P_{01}, of the lowest singlet excited state can be obtained from the absorption spectra by using eq 1 , where $\epsilon(\nu)$ is the

$$P_{01}{}^2 = (9.166 \times 10^{-3}) \int \epsilon(\nu)\, \mathrm{d}\nu/\nu_m \qquad (1)$$

molar extinction coefficient and ν_m is the position of the absorption maximum.[18] The absorption spectra shown in Figure 2 for **1** are not the result of a single transition and therefore must be deconvoluted. We used log-normal curves (GRAMS/32 software) that take into account the asymmetric shape of the absorption band. Compound **1** required five components for a reliable deconvolution whereas **2**, with the same base chromophore, required only a three-component deconvolution. As a result, we have used **2** to determine the transition dipole moment, which, due to its simplified nature, should give more reliable results. The experimental values from eq 1 are shown in Table 1. These values are compared with calculated values determined by a semiempirical method (PM3) that gave electronic states matching two of the three bands found experimentally as shown in Table 1. The correlation between these two bands is satisfactory and the missing transition is assigned to a vibrational band. This latter point is supported by the fact that the third band is shifted from its parent electronic state by 1945 cm^{-1}, which is close to the measured acetylene vibrational frequency of 2207 cm^{-1}.

(17) (a) Zheng, H.; Lai, C. K.; Swager, T. M. *Chem. Mater.* **1994**, *6*, 101. (b) Trzaska, S. T.; Swager, T. M. *Chem. Mater.* **1998**, *10*, 438. (c) Serrette, A. G.; Lai, C. K.; Swager, T. M. *Chem. Mater.* **1994**, *6*, 2252−68.

(18) Turro, N. J. *Modern Molecular Photochemistry*; University Science Books: Sausalito, CA, 1991; Chapter 5.

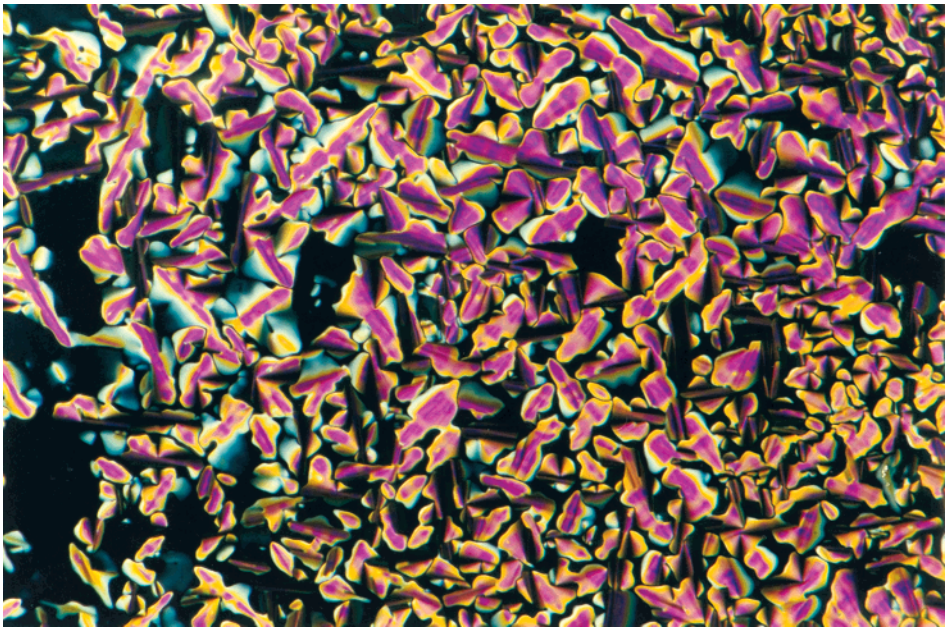

Figure 1. Texture of **1** obtained at 68 °C using a polarizing microscope. The areas of uniform extinction and rectilinear defects are characteristics of a hexagonal columnar phase, Col_h.

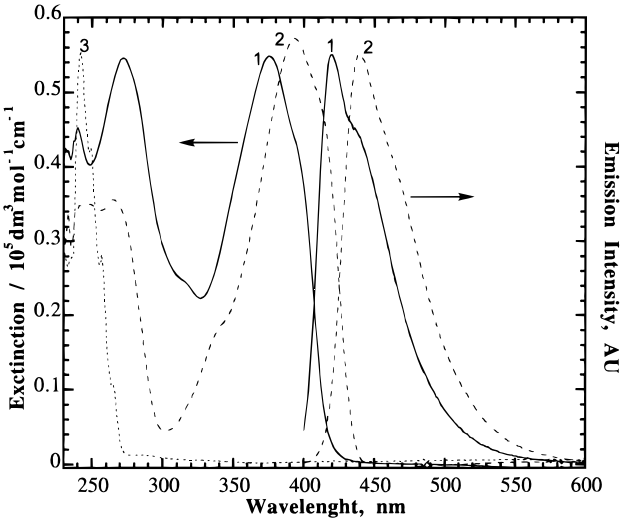

Figure 2. UV−vis spectra of **1**, **2**, and **3** and emission spectra of **1** and **2** taken in a solution of $CHCl_3$.

Scheme 1

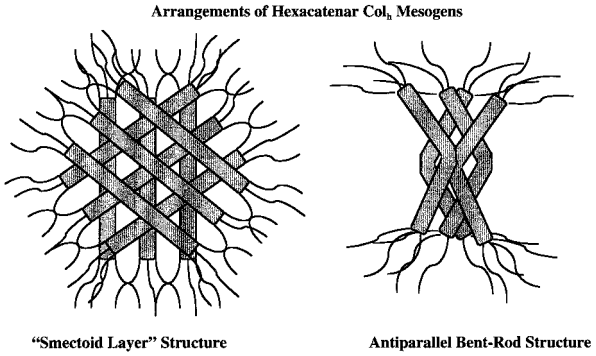

The results of our experimental spectral deconvolution are shown in Figure 3. Comparisons between experimental and calculated transition dipoles in Table 1 indicate that the lowest energy singlet transition has a strong transition dipole of approximately 7.2 D. As no other electronic transitions are close

Table 1. Experimental and Theoretical Absorption Maximum and Transition Dipole Values of **2**

	experiment			PM3 calculations		
band	λ, nm	$\Delta\lambda$,nm	P, D	λ, nm	$\Delta\lambda$,nm	P, D
1	408	0	7.2	417	0	10.8
2	378	30	7.0			
3	336	72	1.5	352	65	3.4

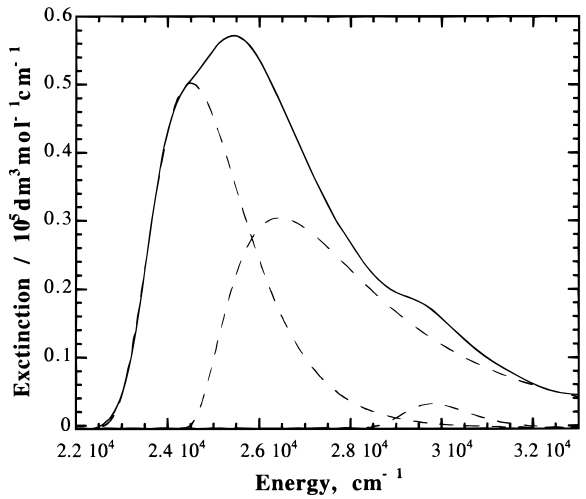

Figure 3. Deconvolution of the absorption spectrum of **2** (solid line) into three log-normal curves (dashed line).

in energy, we need only consider this singular transition in an exciton coupling analysis. Additionally, the PM3 calculations confirm that the transition dipole is principally polarized along the long axis of the molecule.

The fluorescence spectroscopy of **1** in its different phases is shown in Figure 4. These results reveal spectral shifts as well as intensity changes. Figure 5 provides the temperature dependence of λ_{max}, the relative intensity of the peak maximum R_h, and the integral intensity R_i. Simple inspection of these data indicates a clear correlation between the spectroscopic changes and the solid−liquid crystalline and liquid crystalline−isotropic phase transitions. The solid−liquid crystalline phase transition

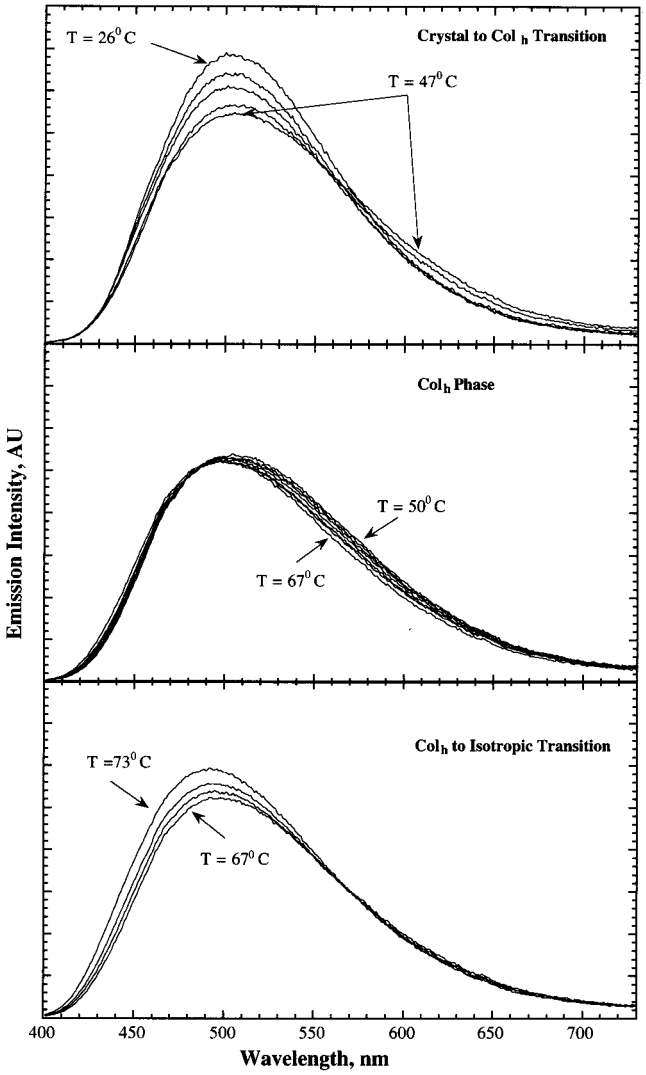

Figure 4. Emission spectra of **1** as a function of temperature (λ_{ex} = 375 nm) The plots shown at the top detail the region of the crystal to Col_h transition, the middle plots show changes within the Col_h phase, and the bottom plots detail the Col_h to isotropic liquid transition.

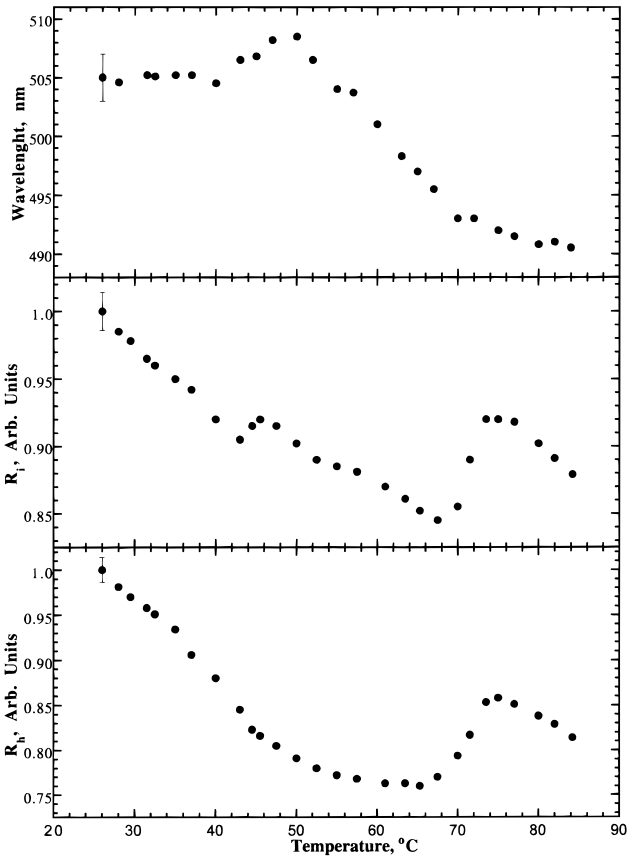

Figure 5. Plots of the emission maximum (nm), the integrated peak intensity R_i, and the peak amplitude R_h of **1** as a function of temperature. The changes at the crystal to Col_h and Col_h to isotropic liquid-phase transitions at 43 and 69 °C, respectively, are readily apparent.

results in a broadening and a red shift of the emission band. Consistent with this broadening, we see a decrease in R_h and an increase in R_i at the solid−liquid crystalline phase transition. Upon heating into the isotropic phase at 69 °C, we observe a distinct blue shift and increase in R_i suggesting a reduction in the ability of the molecules to form self-quenching aggregates. An alternate explanation for the increase in emission efficiency is that the higher organization of the molecules in the liquid crystal phase could facilitate energy transfer to dilute quenching sites dispersed in the material. Hence, it is generally expected for thermally activated radiationless processes that the fluorescence intensity should decrease with increasing temperature.

We are particularly interested in spectroscopic changes which can provide information regarding the intracolumnar correlation of the liquid crystal's mesogenic cores. In this regard, the most interesting feature of our spectroscopic studies is the pronounced blue shift of about 500 cm^{-1} in the columnar mesophase that occurs between ca. 50 and 68 °C. In contrast to the behavior at the phase transitions, over this region the band shape remains unchanged and the integral and peak intensities change proportionally to each other. This static band-shape precludes the possibility that the molecules are undergoing conformational changes to produce the blue shift, since such changes would influence the spectral shape. However, the observations of spectral shape changes at the crystalline−liquid crystalline and the liquid crystalline−isotropic phase transitions are suggestive of concurrent conformation changes.

To analyze the effect of the order and disorder of the liquid crystalline mesogens in the columnar phase, we have applied the exciton model with some special modifications. To begin, it is important to consider the nature of the molecular aggregates of **1**. Based on the large ground-state dipole of **1**, observed Col_h lattice dimensions, and crystallographic studies of a related compound,[4a] it is likely that the molecules are oriented 180° between nearest neighbors. This structure provides a dimeric correlation that approximates a disk shape to provide what we have referred to previously as a discotic antiphase.[17] This structure is also confirmed by computations performed on dimers and trimers of **2**. As shown in Figure 6, the relative energy of the dimer and trimer ground-state structures were calculated (molecular mechanics calculations, Hyperchem software) as a function of the angle of rotation between nearest neighbors while maintaining intermolecular distance of 3.5 Å. The initial position in this plot, $\Phi = 0$, corresponds to a structure with the molecules parallel. In both cases the minimum energy structure is one with the molecules in an antiparallel arrangement between nearest neighbors ($\Phi = 180°$).

We make use of a previously established approach[14] for the simulation of the aggregate fluorescence spectra of **1**. Isolated molecules have strong dipole transition moments (7.2 D), hence the main perturbation to the eigenvalues and eigenfunctions is the off-diagonal exciton coupling terms of the Hamiltonian matrix. For this reason we can simplify our analysis by

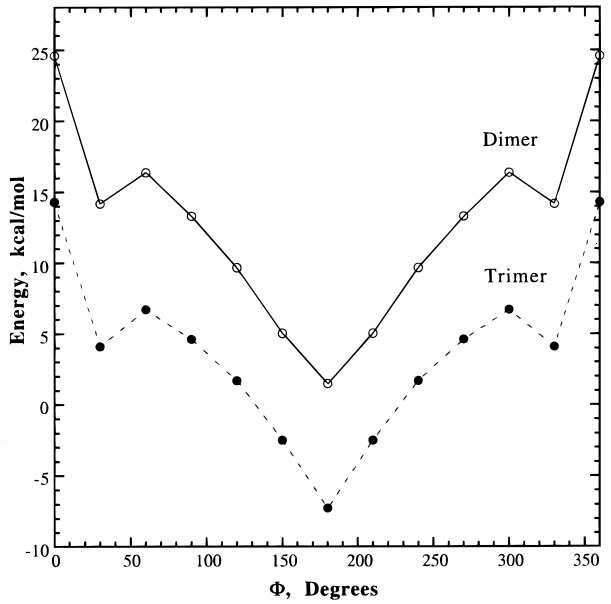

Figure 6. Calculated interaction energies of ground-state dimers and trimers of **2** as a function of rotation angle.

considering that the diagonal terms are negligible. Our model considers an initial aggregate of N flat molecules with antiparallel alignment of dipole moments between neighbor molecules. We then introduce rotational disorder at random angles around the column axis Z. In this case, using the extended dipole model,[19] the off-diagonal terms V_{ij} are given by:

$$V_{ij} = (2q/R_{ij})^2[\{1 + (1/R_{ij})^2 \sin^2(\Delta\beta_{ij}/2)\}^{-1/2} - \{1 + (1/R_{ij})^2 \cos^2(\Delta\beta_{ij}/2)\}^{-1/2}] \quad (2)$$

where R_{ij} is the distance between i and j molecules along the Z axis, $R_{ij} = R_0 \times |j - i|$ (R_0 is spacing of nearest neighbors), $\mathbf{P}_i = q\boldsymbol{l}_i$ is the transition dipole moment for molecule i oriented perpendicular to axis Z, $|\mathbf{P}_i| = P$, $|\boldsymbol{l}_i| = l$, and $\Delta\beta_{ij} = \beta_i - \beta_j$, where β_i and β_j are the angles of $\mathbf{P}_i$ and $\mathbf{P}_j$ with the X-axis, respectively ($\beta_i = 0$ or 180° for ordered molecules in the column). Thus, the Hamiltonian matrix can be defined for known P, R_0, and l values and random rotational angles. A diagonalization of matrix 2 gives eigenvalues (energies) and eigenfunctions for N new collective states. Eigenfunctions $|k>$ and corresponding oscillator strengths f_k for each new state can be found via the following expression: $f_k = (4.68 \times 10^{-7})\epsilon_k \mathbf{P}_k^2$, where ϵ_k and $\mathbf{P}_k$ are the energy (cm^{-1}) and transition dipole moment (D), respectively. The simulation of the fluorescence spectrum was performed assuming that thermal equilibration among $|k>$ states is faster than the radiative rates. Under these circumstances, the Boltzmann factor, $s_k = \exp(-\epsilon_k/k_BT)/\sum \exp(-\epsilon_k/k_BT)$, should be considered for the population of $|k>$ states. The emission spectrum is defined as a superposition of Gaussian curves with areas proportional to $s_k \times f_k$ and a bandwidth equal to the fluorescence band of the molecule in solution (1600 cm^{-1}).

We modeled a column as an aggregate consisting of 36 molecules with an initial antiparallel alignment (ordered organization). This is an adequate model because the position of the peak intensity does not change for $N > 22$ molecules. The stacking distance of 3.5 Å of the mesogen cores is typical in columnar mesophase and was consistent with our X-ray diffraction results. The value of l varied from 10 to 25 Å in accordance with our previous estimations and the dipole transition is 7.2 D. For a given configuration a number of disordered molecules (N_{dis}) randomly distributed among the 36 sites, and for each disordered molecule the angle β_i was defined randomly in the range of 0−360°. The emission spectrum was simulated and averaged over all configurations. The number of configurations varied from 640 to 1200 depending on the strength of the transition dipole interactions, with more configurations being required for systems with large transition dipoles.

The simulated emission spectra for the relatively strong dipole interactions ($l = 10$ Å) and different numbers of disordered molecules are shown in Figure 7. As is seen, an increase in disorder leads to a blue-shift comparable with the experimental observations. More information is presented in Figure 8 where the maxima of the fluorescence bands ν_{max} are plotted against

(19) (a) Czikkely, V.; Försterling, H. D.; Kuhn, H. *Chem. Phys. Lett.* **1970**, *6*, 11. (b) Czikkely, V.; Försterling, H. D.; Kuhn, H. *Chem. Phys. Lett.* **1970**, *6*, 207.

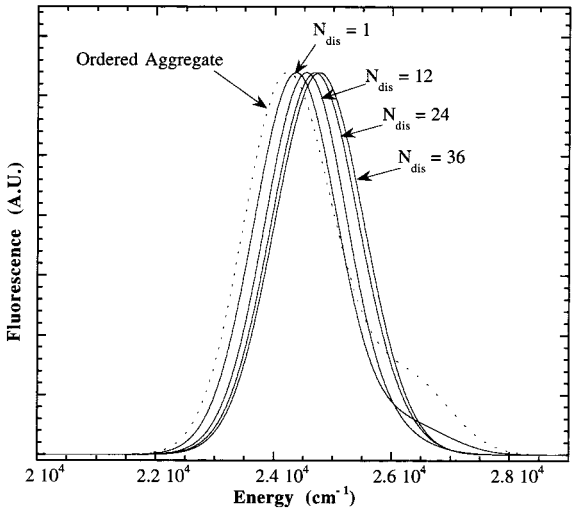

Figure 7. Simulated fluorescence spectrum of a 36 molecule aggregate with different numbers of disordered (N_{dis}) molecules in the aggregate ($P = 7.2$ D, $l = 10$ Å, and stacking distance $R_0 = 3.5$ Å). The dotted line indicates the spectrum of the ordered aggregate with antiparallel molecular alignment.

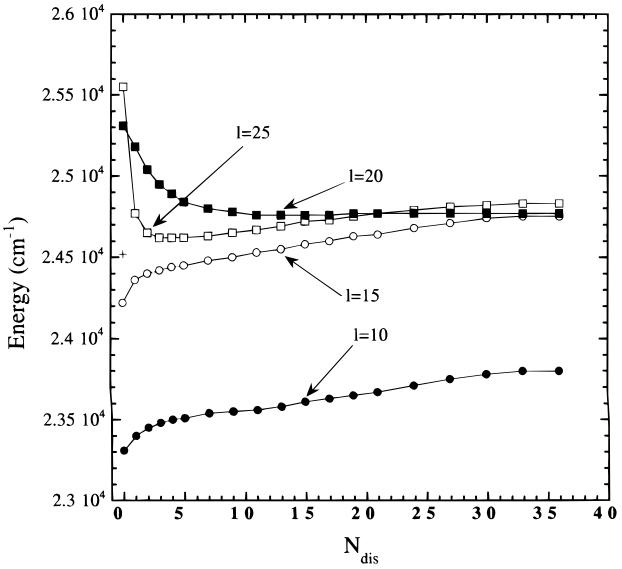

Figure 8. Variation in the calculated position of the fluorescence band on the number of disordered molecules (N_{dis}) for different transition dipole lengths, l ($P = 7.2$ D), and a stacking distance of 3.5 Å. The plus sign marks the energy of an isolated molecule of **1** in solution.

N_{dis} for different values of l. In the case of an ordered aggregate ($N_{dis} = 0$), ν_{max} shifts to lower energy with increasing dipole interactions. The later is expected since a stronger interaction produces greater energy splitting of the aggregate states and subsequently increases the equilibrium population of the lowest states. Note also that the selection rules result in a majority of the oscillator strength being concentrated in the upper states of the ordered aggregate. Therefore, the equilibration will have a considerable influence on the emission spectrum.

Simple inspection of the emission energies as a function of disorder reveals a strong dependence on l. Unfortunately, there is no simple qualitative explanation for the $\nu_{max}(N_{dis})$ dependence at different l values. An increase in the disorder for $l = 25-20$ Å (relatively low to moderate dipole interaction) leads to a red shift for $N_{dis} \leq 5$ and at higher N_{dis} values gives saturation for $l = 25$ Å or a small blue shift for $l = 20$ Å. For relatively strong interactions ($l = 15-10$ Å), the blue shift increases monotonically as N_{dis} increases. The spectral shift between the fully disordered ($N_{dis} = 36$) and minimum disordered ($N_{dis} = 1$) aggregate is similar for $l = 10$ and 15 Å ($\Delta\nu_{max} = 400$ and 380 cm^{-1} respectively). Experimentally, we observe a shift of $\Delta\nu_{max} = 550 \pm 50$ cm^{-1} upon heating from 50 to 66 °C. It is difficult to know the true degree of disorder in the mesophase. Nevertheless, our model provides the correct direction and order of magnitude of the fluorescence spectral shift with increasing disorder in the columnar aggregate.

Conclusion

In summary, we have illustrated the application of exciton coupling in the analysis of the intermolecular correlations of a novel bent-rod hexacatenar liquid crystal with a large lateral dipole. The exciton coupling combined with modeling the disorder presents a method that could be used to complement other established methods to analyze pairwise distributions in highly anisotropic dipolar liquid crystals. Our results support our assignment of a new antiparallel organization of nearest neighbor bent-rod mesogens in a hexacatenar Col_h phase (Scheme 1). This structure also presents interesting possibilities for the creation of biaxial character in hexagonal columnar phases. The study of energy transfer dynamics and extended electronic interaction in liquid crystals is continuing to gain importance for the design of functional supramolecular assemblies and devices. Hence, these methods should be useful for the analysis of future generations of liquid crystalline systems.

Experimental Section

General Methods. ^{1}H NMR spectra were recorded on a Varian Unity VXR 500. Chemical shifts are reported in ppm relative to residual $CHCl_3$ ($\delta = 7.24$, ^{1}H). Multiplicities are given as s (singlet), d (doublet), t (triplet), and m (multiplet). MS investigations were run on a Finnigan MAT 8200 equipped with an Ion Tech ion source. Optical characterization was performed on a Leica DMRXP polarizing microscope equipped with a Wild Leitz MPS46 Photoautomat along with a Linkam LTS 350 hot stage and a Linkam TP 92 controller. Transition temperatures and heats of fusion were determined at scan rates of 10 deg C/min by differential scanning calorimetry using a Perkin-Elmer DSC 7 with a Perkin-Elmer Pyris thermal analysis data station. Variable-temperature X-ray measurements were performed on an Inel system (CPS 120 detector, XRG 2000 generator, Cu Kα radiation, Minco CT 137 temperature controller (±1 °C) and a home-built heating stage) as well as a Siemens system (flat camera 2D-Xe-detector, 256 × 256 cells, Instec HS 400 hot stage and STC 200 controller, Rigaku RU-−H3R rotating anode, Ni-filtered Cu Kα radiation). Calibration was accomplished by using mica and silicon standards (NBS). Samples were prepared by filling each Lindemann capillary (1.5 mm) with approximately 15 mg of compound. UV−vis spectra were obtained from a Hewlett-Packard 8452A diode array spectrophotometer. Fluorescence studies were conducted with a SPEX Fluorolog-τ2 fluorometer (model FL112, 450 W xenon lamp). All emission and excitation spectra were corrected for the detector response and the lamp output. For all spectra an excitation wavelength of 375 nm was used. Thin-film spectra of the various phases were recorded by front-face (22.5°) detection. These films were prepared from an isotropic melt of **1** between two microscope cover slips. The temperature of the sample was controlled by a Neslab RTE-111 thermostated recirculation unit. The solution studies were performed at a concentration of 10^{-5} M in spectroscopic grade chloroform. Unless otherwise indicated, all chemicals and solvents were purchased commercially and used as obtained without further purification. Dichloromethane was freshly distilled from CaH_2 under an atmosphere of dry argon. 2,5-Bis[(4-hydroxyphenyl)ethynyl]-3,4-dicyanothiophene and 3,4,5-tridodecyloxybenzoic acid were synthesized following literature procedures.[5,20]

2,5-Bis[4-(3,4,5-tridodecyloxyphenylcarbonyloxy)phenylethynyl]-3,4-dicyanothiophene (1). 2,5-Bis[(4-hydroxyphenyl)ethynyl]-3,4-dicyanothiophene (40.0 mg, 0.109 mmol), 3,4,5-tridodecyloxybenzoic acid (148 mg, 0.218 mmol), and 4-(dimethylamino)pyridine (2.66 mg, 0.022 mmol) were dissolved in dry dichloromethane (10 mL) under argon. A solution of *N*,*N*′-diisopropylcarbodiimide (30.3 mg, 0.240 mmol) in dry dichloromethane (5 mL) was added and the mixture was stirred for 24 h. Aqueous HCl (1 M, 10 mL) was added and the mixture was stirred for another 15 min. The organic components were extracted with dichloromethane, and the combined organic phases were dried over $MgSO_4$, concentrated, and finally chromatographed on silica gel using dichloromethane as eluent to give **1** as a yellow solid (97.7 mg, 53%). For analytical measurements, a further purification was achieved when **1** was precipitated from a concentrated THF solution by the addition of methanol. ^{1}H NMR ($CDCl_3$, δ): 7.68 (d, $J = 8.4$ Hz, 4H, Ar H), 7.34 (s, 4H, Ar H), 7.28 (d, $J = 8.4$ Hz, 4H, Ar H), 4.05 (m, 12H, OCH_2), 1.84 (m, 12H, OCH_2CH_2), 1.49 (m, 12H, CH_2), 1.27 (m, 96H, CH_2), 0.88 (t, 18H, CH_3). IR (KBr, thin film) ν_{max} (cm^{-1}): 2229 (C≡N), 2209 (C≡N, C≡C), 1726 (C═O). MS-FAB *m*/*z* (rel intensity): 1680.0 (72.0, $[M + H]^+$), 1678.9 (100, M^+). HRMS-FAB (*m*/*z*): $[M + H]^+$ calcd for $C_{108}H_{162}N_{20}O_{10}S$ 1679.1950, found 1679.1925 ± 0.0048.

Acknowledgment. We are grateful for the generous financial support from the Office of Naval Research, NEDO, and the National Science Foundation. This work made use of equipment provided by the MRSEC Program of the National Science Foundation under award No. DMR 98-08941.

JA993947D

(20) Meier, H.; Prass, E.; Zerban, G.; Kosteyn, F. *Z. Naturfroch*. **1988**, *43*, 889.